Available online at www.sciencedirect.com
ScienceDirect
Journal of Photochemistry and Photobiology A: Chemistry 197 (2008) 232–238
Journal of Photochemistry and Photobiology A:Chemistry
www.elsevier.com/locate/jphotochem

UV direct photolysis of 2,2′-azino-bis(3-ethylbenzothiazoline-6-sulfonate) (ABTS) in aqueous solution: Kinetics and mechanism

Changha Lee, Jeyong Yoon *

School of Chemical and Biological Engineering, College of Engineering, Seoul National University, San 56-1, Sillim-dong, Gwanak-gu, Seoul 151-742, Republic of Korea

Received 3 September 2007; received in revised form 13 December 2007; accepted 26 December 2007
Available online 5 January 2008

Abstract

The direct photolysis of 2,2′-azino-bis(3-ethylbenzothiazoline-6-sulfonate) (ABTS) in aqueous solution was investigated under monochromatic ultraviolet (UV) irradiation at 254 nm. ABTS was found to be directly photolyzed by UV irradiation to yield the one-electron oxidized radical, $ABTS^{\bullet+}$, which is a blue-green colored persistent radical species that has strong visible absorption bands. The photochemical production of $ABTS^{\bullet+}$ was strongly dependent on the solution pH and the presence of dissolved oxygen. The presence of dissolved oxygen increased the quantum yields at pH 3, whereas it inhibited the production of $ABTS^{\bullet+}$ at pH 6.5. Spectrophotometric and spectrofluorometric data indicated that ABTS photolysis may occur as a result of the transfer of one-electron between the singlet excited state and the ground state of ABTS. Observations made during UV/H_2O_2 experiments with ABTS suggested that the dependence of the photoloysis of ABTS on the solution pH and the presence of dissolved oxygen is related to the role of the hydroperoxyl/superoxide radical ($HO_2^{\bullet}/O_2^{\bullet-}$), which appears to be formed via a secondary reaction of the reduced intermediate of ABTS with dissolved oxygen. The proposed photolytic reactions were supported by the observed stoichiometry between the amount of $ABTS^{\bullet+}$ radicals produced and the amount of ABTS molecules decomposed.

Keywords: ABTS; Photolysis; Ultraviolet irradiation; Photooxidation

1. Introduction

2,2′-Azino-bis(3-ethylbenzothiazoline-6-sulfonate) (ABTS) is a well-known compound used for the colorimetric analysis of various chemical oxidants. The colorless ABTS molecule is converted to the blue-green colored radical, $ABTS^{\bullet+}$, by oxidation of one-electron, as depicted in Fig. 1. $ABTS^{\bullet+}$ shows strong UV–vis absorption bands centered at 415, 648, 728 and 812 nm, and is known to be a persistent radical species.

It has been reported that $ABTS^{\bullet+}$ can be rapidly formed by reactions of ABTS with various inorganic radicals, such as $^{\bullet}OH$, $Br_2^{\bullet-}$ and $RS^{\bullet}$ [1,2], and various organic radicals, such as alkoxyl or alkoxylperoxyl radicals [3,4]. In addition, non-radical oxidants, such as percarboxylic acid [5], ferrate [6], bromine and chlorine species [7], are known to react with ABTS to stoichiometrically produce $ABTS^{\bullet+}$. Therefore, ABTS has been used as a kinetic probe for the study of free radical reactions, as well as a reagent for the quantitative analysis of chemical oxidants.

Although the formation of $ABTS^{\bullet+}$ by chemical oxidation is well-documented, there has been only one study conducted that has reported the photolytic formation of $ABTS^{\bullet+}$ radicals. Maruthamuthu et al. has reported that ABTS is oxidized to $ABTS^{\bullet+}$ as a photosensitizer of UV-illuminated TiO_2 suspension [8]. In this study, we observed the direct photolysis of ABTS to $ABTS^{\bullet+}$ under UV irradiation at 254 nm for the first time. The effects of solution pH and dissolved oxygen on the photochemical production of $ABTS^{\bullet+}$ were investigated, and their photochemical mechanisms are discussed based on the spectrophotometric and spectrofluorometric data. The photochemical formation of the blue-green colored radical, $ABTS^{\bullet+}$, can be used as a simple chemical actinometry system.

* Corresponding author. Tel.: +82 2 880 8927; fax: +82 2 876 8911.
E-mail address: jeyong@snu.ac.kr (J. Yoon).

1010-6030/$ – see front matter © 2008 Elsevier B.V. All rights reserved.
doi:10.1016/j.jphotochem.2007.12.030

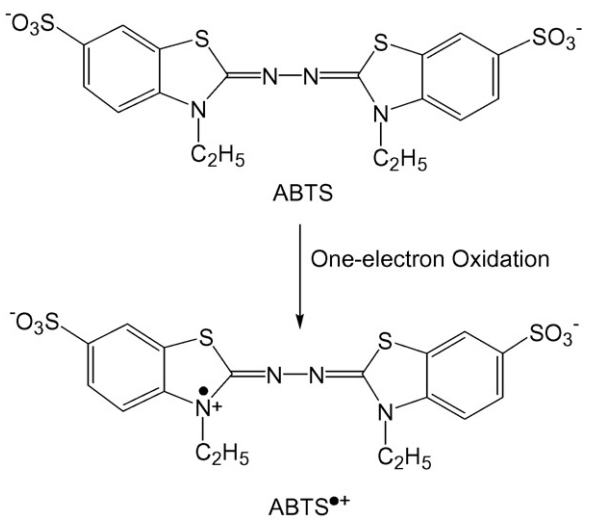

Fig. 1. ABTS and its one-electron oxidation product, $ABTS^{\bullet+}$.

2. Experimental

2.1. Reagents

All of the chemicals used were of reagent grade and were used without further purification. ABTS diammonium salt, sodium hydroxide, perchloric acid and potassium persulfate were purchased from Aldrich Co. All water used was distilled and deionized (Barnstead NANO Pure). A 35% aqueous solution of hydrogen peroxide (H_2O_2) was obtained from Fluka Co. The stock solutions of the ABTS reagent were prepared by dissolving 1 g of ABTS diammonium salt in 1 L distilled water (1.8 mM), which was then stored at 4 °C in the dark by covering the containers with aluminum foil. The ABTS stock solution was spectrophotometrically checked for variance prior to use. For some experiments, $ABTS^{\bullet+}$ was prepared by mixing an ABTS stock solution with potassium persulfate, which was then stored at 4 °C in the dark [9].

2.2. Experimental apparatus and procedure

All experiments were performed in a 150 ml Pyrex reactor with a quartz window that allowed the solution to be exposed to the UV irradiation from a 13 W low-pressure mercury vapor lamp (TUV 13 W, 99% emission at 254 nm, Philips Co.). The optical path length of this system was chemically determined to be 3.5 cm using the photolysis kinetics of H_2O_2 [10]. For experiments in which gas sparging was conducted, the top of the reactor was sealed with a rubber septum, and O_2 or N_2 bubbling was then performed using a needle-type diffuser. The incident photon flow (Einstein l^{-1} s^{-1}) was measured using ferrioxalate actinometry [11], and the photolytic production of Fe(II) was kept at <10% of the initial amount of Fe(III) to ensure complete light absorption by the ferrioxalate actinometer. An overall quantum yield of 1.2 was used in the calculation pertaining to the ferrioxalate photolysis reaction [12].

The general experimental procedure was as follows: an ABTS solution with a specific concentration was prepared by adding a calculated aliquot of ABTS stock solution to distilled water. The initial pH of the ABTS solution was around 6.5, however, the solution pH increased slightly to 6.8 ± 0.2 as a result of the reaction. For some experiments in acidic pH conditions, the initial pH of the solutions was adjusted as 3 by adding appropriate amounts of 0.1N $HClO_4$. No variation in the solution pH was observed during the reaction time at pH 3. The prepared solution in the reactor was placed in a thermostat, in order to maintain the solution temperature at 25 ± 0.5 °C. The photolysis was initiated upon exposing the reactor to the UV irradiation. Samples were withdrawn at predetermined timed intervals and rapidly analyzed immediately after the sampling. In most of the experiments, a set of triplicate photolysis experiments was carried out, and then the average values and the standard deviations were presented.

2.3. Analysis

The analyses of Fe(II) for ferrioxalate actinometry were carried out using the 1,10-phenanthroline method [13]. The pH measurements were carried out with an Orion 710A pH-meter, which was calibrated with standard buffer solutions. UV–vis absorption spectra were obtained using a Hewlett-Packard 8453 diode array spectrophotometer, and fluorescence spectra were obtained using a JASCO FP-6500 spectrofluorometer. A quartz cell with a path length of 1 cm was used for spectrophotometric and spectrofluorometric measurements.

3. Results and discussion

3.1. Production of $ABTS^{\bullet+}$ by ABTS photolysis

The UV direct photolysis of ABTS under UV irradiation at 254 nm in a deaerated aqueous solution was investigated. As shown in Fig. 2, the colorless ABTS solution gradually turned blue-green during the photolysis. The intensity of the UV absorption band of ABTS at 340 nm gradually decreased, whereas those of the visible absorption bands centered at 415, 648, 728 and 812 nm increased as the reaction proceeded, indicating that ABTS is decomposed to produce $ABTS^{\bullet+}$ as a result of direct photolysis.

Based on the measured variations in the absorbance of the ABTS solution at 340 and 415 nm (ΔA_{340} and ΔA_{415}), the concentrations of the $ABTS^{\bullet+}$ radicals produced and the ABTS molecules decomposed were calculated by the following equations using the known molar absorption coefficients of ABTS at 340 nm ($\varepsilon_{ABTS^{\bullet+},340} = 3.66 \times 10^4\ M^{-1}\ cm^{-1}$) and $ABTS^{\bullet+}$ at 340 and 415 nm ($\varepsilon_{ABTS^{\bullet+},340} = 1.33 \times 10^4\ M^{-1}\ cm^{-1}$; $\varepsilon_{ABTS^{\bullet+},415} = 3.40 \times 10^4\ M^{-1}\ cm^{-1}$) [14].

$$\text{produced } ABTS^{\bullet+} : [ABTS^{\bullet+}] = \frac{\Delta A_{415}}{\varepsilon_{ABTS^{\bullet+},415}} \quad (1)$$

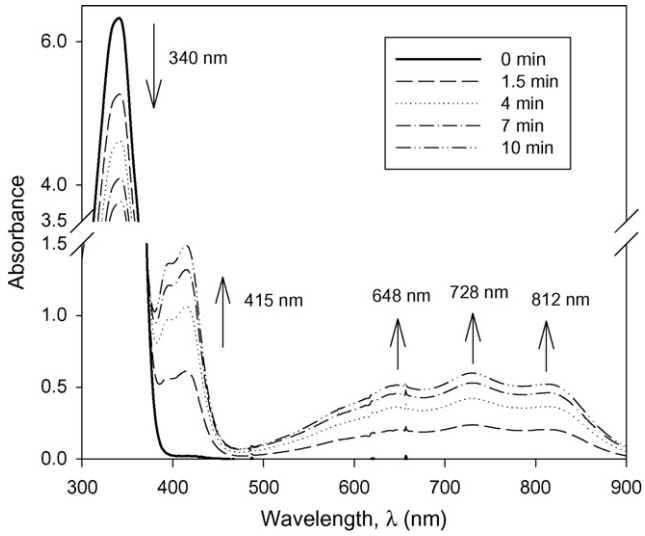

Fig. 2. Variation in the UV–vis spectrum of the ABTS solution during UV irradiation ($[ABTS]_0 = 1.8 \times 10^{-4}$ M, pH$_0$ 6.5, $I = 1.52 \times 10^{-6}$ Einstein l^{-1} s^{-1}, N_2 gas purging).

$$\text{decomposed ABTS} : \Delta[ABTS] = [ABTS]_0 - [ABTS] = \frac{\Delta A_{340} - \varepsilon_{ABTS^{\bullet+},340}[ABTS^{\bullet+}]}{\varepsilon_{ABTS,340}} \quad (2)$$

Fig. 3a shows the concentration–time profiles of the $ABTS^{\bullet+}$ radicals produced ($[ABTS^{\bullet+}]$) and the ABTS concentration decomposed ($\Delta[ABTS]$) during the ABTS photolysis. Both $[ABTS^{\bullet+}]$ and $\Delta[ABTS]$ increased with increasing UV irradiation time. A plot of $\Delta[ABTS]$ against $[ABTS^{\bullet+}]$ (Fig. 3b) revealed a perfect linear curve with a slope of 1.95 (≈2), which suggests that two moles of ABTS are decomposed to produce one mole of $ABTS^{\bullet+}$.

3.2. Mechanism for the photolysis of ABTS to $ABTS^{\bullet+}$

The proposed simplest mechanism of ABTS photolysis is described by reactions (3)–(6). According to reaction (5), the photo-excited state of ABTS ($ABTS(S_1)$) takes one-electron from the ground state of ABTS molecule to produce $ABTS^{\bullet+}$. The reduced form of ABTS ($ABTS^{\bullet-}$) may be decomposed to form the unknown product, P_1 (reaction (6)). Overall, two moles of ABTS are consumed to produce one mole of $ABTS^{\bullet+}$ (reaction (7)). Additionally, analysis of the emission spectra of ABTS verified that the spin multiplicity of the photo-excited state of ABTS is a singlet. A wide fluorescence band raging from 370 to 600 nm with a λ_{max} around 475 nm was obtained (Fig. 4), which agrees with the results of a previous study [8]. The phosphorescence spectrum of ABTS in the deaerated aqueous solution was not observed.

$$ABTS + h\nu \rightarrow ABTS(S_1) \quad (3)$$

$$ABTS(S_1) \rightarrow ABTS + h\nu' \quad (4)$$

$$ABTS(S_1) + ABTS \rightarrow ABTS^{\bullet+} + ABTS^{\bullet-} \quad (5)$$

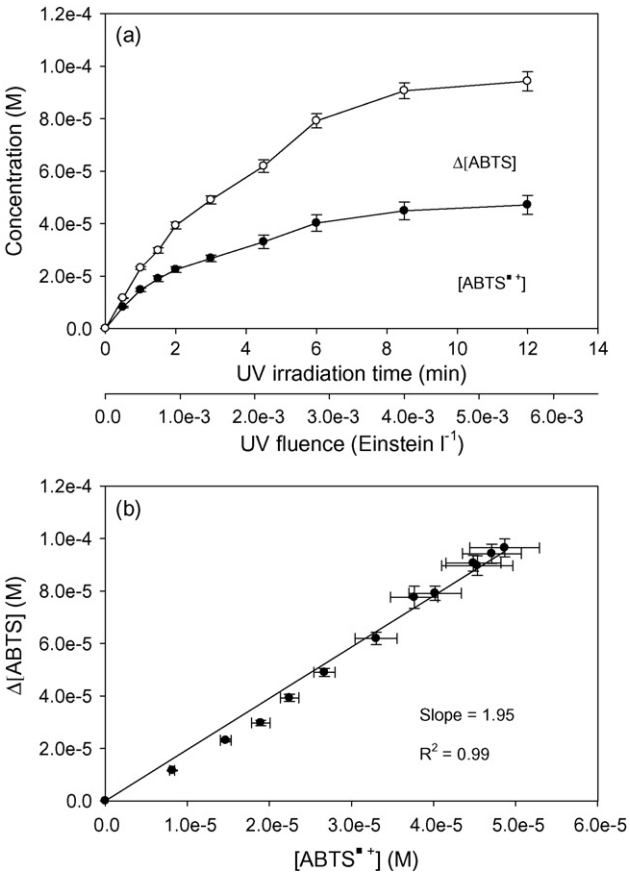

Fig. 3. (a) Concentration–time (UV fluence) profiles of $ABTS^{\bullet+}$ produced and ABTS decomposed during ABTS photolysis and (b) stoichiometry between them ($[ABTS]_0 = 1.8 \times 10^{-4}$ M, pH 6.5, $I = 1.52 \times 10^{-6}$ Einstein l^{-1} s^{-1}, N_2 gas purging).

$$ABTS^{\bullet-} \rightarrow \rightarrow P_1 \quad (6)$$

$$\text{Net} : 2ABTS + h\nu \rightarrow ABTS^{\bullet+} + P_1 \quad (7)$$

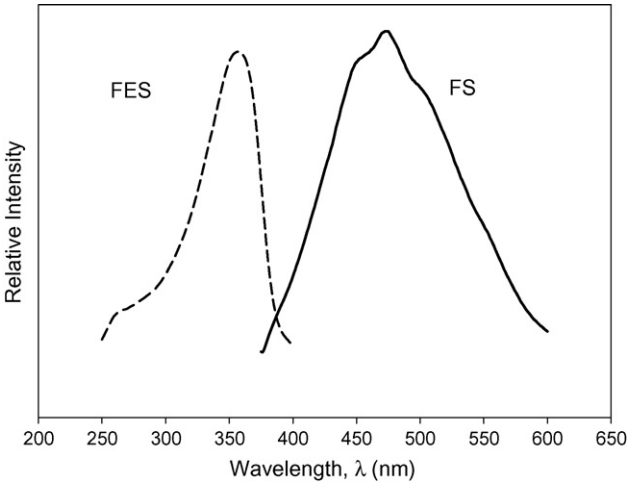

Fig. 4. Fluorescence spectrum (FS) and fluorescence excitation spectrum (FES) of ABTS in aqueous solution (for FS, $[ABTS]_0 = 1.8 \times 10^{-4}$ M, excitation wavelength = 360 nm; for FES, $[ABTS]_0 = 1.8 \times 10^{-5}$ M, excitation wavelength = 250–400 nm, monitoring wavelength = 475 nm).

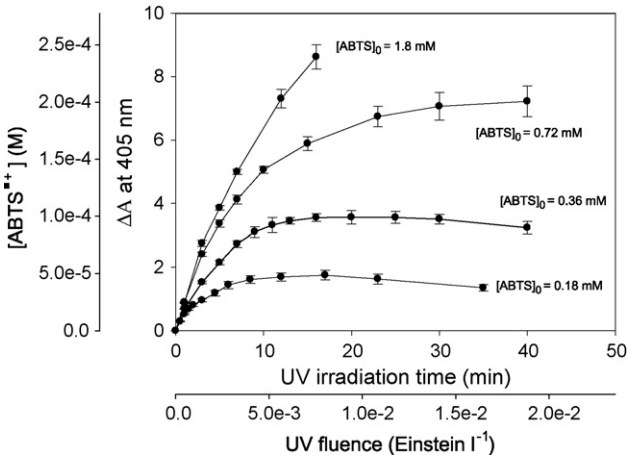

Fig. 5. Concentration–time (UV fluence) profiles of $ABTS^{\bullet+}$ produced during ABTS photolysis when various initial concentrations of ABTS were used (pH 6.5, $I = 1.52 \times 10^{-6}$ Einstein l^{-1} s^{-1}, N_2 gas purging).

The results of Figs. 5 and 6 strongly support the proposed reaction between $ABTS(S_1)$ and ABTS. As shown in Fig. 5, the rate at which ABTS photolysis to $ABTS^{\bullet+}$ occurs was enhanced by increasing the initial concentration of ABTS ($[ABTS]_0$) from 1.8×10^{-4} to 1.8×10^{-3} M. However, this cannot occur as a result of enhanced photon absorption by ABTS. Because, based on the molar absorption coefficient of ABTS at 254 nm

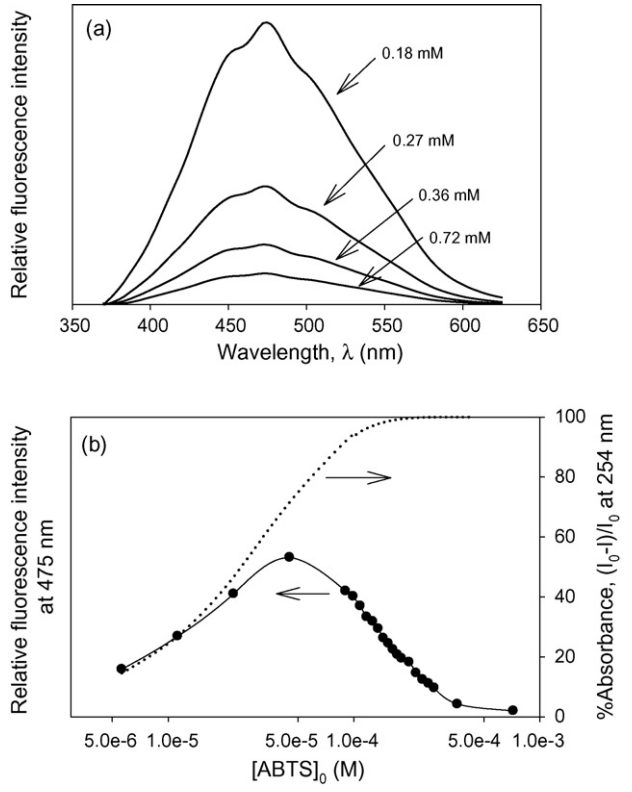

Fig. 6. (a) Fluorescence spectra of ABTS when various initial concentrations of ABTS were used and (b) relative fluorescence intensity at 475 nm as a function of ABTS concentration (excitation wavelength = 254 nm, the dotted line indicates UV absorbance by ABTS at 254 nm calculated using $\varepsilon_{ABTS,254} \approx 1.9 \times 10^4$ M^{-1} cm^{-1} and $L = 1$ cm).

($\varepsilon_{ABTS,254} \approx 1.9 \times 10^4$ M^{-1} cm^{-1}) and the optical path length of the reactor (3.5 cm), all of the incident photons (>99%) can be absorbed by ABTS only if $[ABTS]_0 > 3 \times 10^{-5}$ M. The enhanced production of $ABTS^{\bullet+}$ in this region of $[ABTS]_0$ is due to the enhancement of reaction (5). The photo-excited state ($ABTS(S_1)$) relaxes to its ground state by emitting fluorescence (reaction (4)) unless it reacts with ABTS (reaction (5)). Increasing $[ABTS]_0$ accelerates the rate of reaction (5).

In addition, the fluorescence spectra of ABTS as a function of $[ABTS]_0$, as shown in Figs. 6a and b, confirm the quenching of fluorescence by ABTS (competition between reactions (4) and (5)). Fig. 6a shows that the fluorescence intensity of ABTS significantly decreases as $[ABTS]_0$ increases from 1.8×10^{-4} to 7.2×10^{-3} M. Fig. 6b shows a comparison of the fluorescence intensity at 475 nm (symbols) and the calculated UV absorbance by ABTS at 254 nm (dotted line) as a function of $[ABTS]_0$. The intensity of fluorescence increases in the region of low ABTS concentration as a result of the increasing photon absorption by ABTS, whereas it starts to decrease around the point at which $[ABTS]_0 > 5 \times 10^{-5}$ M, most likely as a result of the consumption of $ABTS(S_1)$ by ABTS, as described in reaction (5) (fluorescence quenching by ABTS).

The fluorescence lifetime should be dependent on $[ABTS]_0$ because of reaction (5). Maruthamuthu et al. observed that the lifetime of $ABTS(S_1)$ (τ_f) was ~80 ps at $[ABTS]_0 = 2.75 \times 10^{-4}$ M using picosecond pulsed-laser spectroscopy [8]. By fitting this value and the data in Fig. 6b into the kinetic equations derived from reactions (3)–(5), the rate constants for reactions (4) and (5) (k_4 and k_5) were determined to be 1.8×10^9 s^{-1} and 3.8×10^{13} M^{-1} s^{-1}, respectively. In addition, based on the determined rate constants, τ_f was calculated to be 0.54 ns to 24 ps at $[ABTS]_0 = 1 \times 10^{-6}$ to 1×10^{-3} M. Details for the calculation are described in supplementary data, S-1.

3.3. Effects of solution pH and dissolved oxygen

The effect of dissolved oxygen on the photolysis of ABTS to $ABTS^{\bullet+}$ was investigated using solutions with two different pH levels (Fig. 7a and b). To obtain linear UV fluence–concentration profiles of $ABTS^{\bullet+}$, a high concentration of ABTS (1.8×10^{-3} M) was used and the photolytic production of $ABTS^{\bullet+}$ was kept at <1.5% of the initial amount of ABTS, which ensured that complete light absorption by ABTS occurred. The quantum yields (ϕ) of the photochemical production of $ABTS^{\bullet+}$ were then determined from the slopes of linear plots. Interestingly, when the solution used had a pH of 6.5, O_2 saturation decreased the ϕ value by 70% from 4.75×10^{-2} to 1.47×10^{-2} (Fig. 7a), whereas it increased the value by 70% from 3.37×10^{-2} to 5.68×10^{-2} when a solution with a pH 3 was used (Fig. 7b). The difference of the ϕ values at pH 3 and 6.5 under N_2 condition appears to be due to the protonation of ABTS (pK_a of $HABTS^+ = 2.08$) [14].

As shown in proposed reactions (3)–(6), the only potential species that dissolved oxygen can interact with are $ABTS(S_1)$ and $ABTS^{\bullet-}$, since ABTS and $ABTS^{\bullet+}$ are stable when in an aqueous solution containing dissolved oxygen. However, the fluorescence spectra of ABTS was constant regardless of the

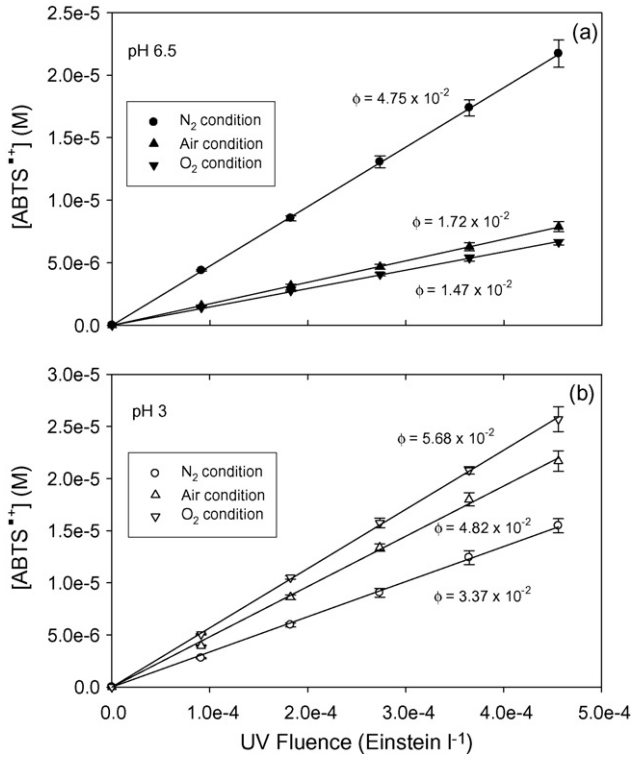

Fig. 7. Effect of dissolved oxygen on the production of $ABTS^{\bullet+}$ during ABTS photolysis (a) at pH 6.5 and (b) at pH 3 ($[ABTS]_0 = 1.8 \times 10^{-3}$ M, $[ABTS^{\bullet+}] < 2.7 \times 10^{-5}$ M (1.5% of $[ABTS]_0$), $I = 1.21 \times 10^{-7}$ Einstein l^{-1} s^{-1}).

presence of dissolved oxygen (data not shown), indicating that no significant reaction between ABTS(S_1) and oxygen occurs. Therefore, $ABTS^{\bullet-}$ is the only species that can be responsible for the reaction with dissolved oxygen, which suggests that $ABTS^{\bullet-}$ transfers one-electron into dissolved oxygen to yield a superoxide radical ($O_2^{\bullet-}$), as described in reaction 8. At a pH <4.8, $O_2^{\bullet-}$ is protonated to yield a hydroperoxyl radical ($HO_2^{\bullet}$).

$$ABTS^{\bullet-} + O_2 \rightarrow ABTS + O_2^{\bullet-} \quad (8)$$

$$O_2^{\bullet-} + H^+ \rightarrow HO_2^{\bullet} \qquad pK_a = 4.8 [15] \quad (9)$$

The dual behaviors of $HO_2^{\bullet}/O_2^{\bullet-}$ proposed in the following reactions explain the opposite effects of dissolved oxygen on the photochemical production of $ABTS^{\bullet+}$ at pH 6.5 and 3 (Figs. 7a and b). At pH 6.5, $O_2^{\bullet-}$ may preferentially reduce $ABTS^{\bullet+}$ into ABTS, lowering the quantum yield for $ABTS^{\bullet+}$ production (reaction (10)). Conversely, at pH 3, it may be favorable for $HO_2^{\bullet}$ to oxidize another ABTS molecule to yield $ABTS^{\bullet+}$, which in turn increases the quantum yield (reaction (11)). Similar behaviors of $HO_2^{\bullet}/O_2^{\bullet-}$ have been reported in reactions involving metal ions, such as Fe(II)/Fe(III) and Cu(I)/Cu(II). According to the reported rate constants [15], $O_2^{\bullet-}$ favorably reduces Fe(III) and Cu(II) to Fe(II) and Cu(I), respectively, whereas $HO_2^{\bullet}$ preferentially leads to their reverse oxidation reactions.

$$ABTS^{\bullet+} + O_2^{\bullet-} \rightarrow ABTS + O_2 \qquad pH6.5 \quad (10)$$

$$ABTS + HO_2^{\bullet} \rightarrow ABTS^{\bullet+} + HO_2^- \qquad pH3 \quad (11)$$

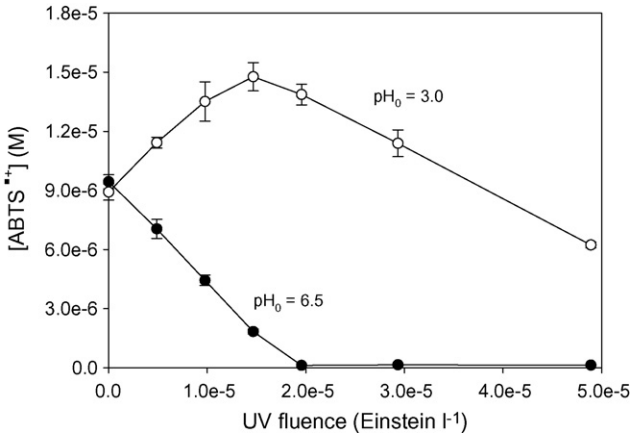

Fig. 8. Concentration–UV fluence profiles of $ABTS^{\bullet+}$ in the UV/H_2O_2 system ($[H_2O_2]_0 = 0.2$ M, $[ABTS]_0 = [ABTS^{\bullet+}]_0 = 9 \times 10^{-6}$ M, $I = 1.21 \times 10^{-7}$ Einstein l^{-1} s^{-1}).

In order to verify the dual roles of $HO_2^{\bullet}/O_2^{\bullet-}$ (reactions (10) and (11)), a UV/H_2O_2 system that had an excess amount of H_2O_2 (0.2 M) was employed using solutions with a pHs 3 and 7 to produce $HO_2^{\bullet}$ and $O_2^{\bullet-}$, respectively (Fig. 8). The reaction solution was spiked with equivalent concentrations of ABTS and $ABTS^{\bullet+}$ ($[ABTS]_0 = [ABTS^{\bullet+}]_0 \approx 9 \times 10^{-6}$ M), and the variation of $[ABTS^{\bullet+}]$ with irradiation time was measured. In aqueous solution, UV irradiation splits H_2O_2 into two hydroxyl radicals ($^{\bullet}OH$) with a quantum yield of unity ($\phi_{^{\bullet}OH} = 1$) [16,17]. The hydroxyl radicals subsequently react with H_2O_2 to produce $HO_2^{\bullet}$ in the presence of excess H_2O_2, as described in the following reaction:

$$H_2O_2 + {}^{\bullet}OH \rightarrow HO_2^{\bullet} + H_2O$$

$$k_{12} = 2.7 \times 10^7\ M^{-1}\ s^{-1} [18] \quad (12)$$

Based on the molar absorption coefficients of H_2O_2 ($\varepsilon_{ABTS,254} = 19.6\ M^{-1}\ cm^{-1}$ [19]) and ABTS ($\varepsilon_{ABTS,254} \approx 1.9 \times 10^4\ M^{-1}\ cm^{-1}$ [14]) at 254 nm, as well as the concentrations of H_2O_2 (0.2 M) and ABTS (9×10^{-6} M) in the solution in Fig. 8, it was determined that more than 95% of the incident photons are absorbed by H_2O_2. Furthermore, considering the significantly higher quantum yield of the photolysis of H_2O_2 (≈1) than that of ABTS (1.72–5.68 × 10^{-2} in Fig. 7a and b), $ABTS^{\bullet+}$ generation as a result of the direct photolysis of ABTS can be completely neglected.

The results in Fig. 8 clearly show the dual roles of $HO_2^{\bullet}/O_2^{\bullet-}$ when solutions of different pH are used. In the initial stage of the reaction, $[ABTS^{\bullet+}]$ linearly increased in response to UV irradiation at pH 3, whereas it decreased at the same rate at pH 6.5, which supports the mechanism proposed in reactions (10) and (11). $[ABTS^{\bullet+}]$ at pH 3 began to decrease after being exposed to 1.5×10^{-5} Einstein l^{-1} of UV fluence, suggesting that $ABTS^{\bullet+}$ can be transformed into the secondary oxidized product as a result of further reaction with $HO_2^{\bullet}$. The variations in the UV–vis spectrum during the reaction confirmed that the latter decrease of $[ABTS^{\bullet+}]$ at pH 3 is not due to the reverse reaction of $ABTS^{\bullet+}$ into ABTS (refer to supplementary data, S-2).

3.4. Stoichiometry

The proposed photolytic reactions involving the effects of dissolved oxygen and solution pH can also be verified by investigating the stoichiometry between the amounts of $ABTS^{\bullet+}$ radicals produced ($[ABTS^{\bullet+}]$) and the amount of ABTS molecules decomposed ($\Delta[ABTS]$) during ABTS photolysis. According to the proposed mechanisms (reactions (3)–(11)), the theoretical stoichiometric factors for the photochemical conversion of ABTS to $ABTS^{\bullet+}$ ($\Delta[ABTS]/[ABTS^{\bullet+}]$) in three different conditions; pH 6.5, N_2 (condition 1), pH 3, N_2 (condition 2) and pH 6.5, O_2 (condition 3), should be 2, since two moles of ABTS are decomposed to produce one mole of $ABTS^{\bullet+}$ (refer to reaction (7) for conditions 1 and 2, and supplementary data, S-3 for condition 3).

Conversely, the theoretical stoichiometric factor when a solution with a pH 3 that contains O_2 is used (condition 4) should be between 1 and 2, depending on the competitive contributions of reactions (6) and (8). Based on the fact that O_2 saturation affected the ϕ value by approximately 70% (70% decrease at pH 6.5 in Fig. 7a; 70% increase at pH 3 in Fig. 7b), it can be determined that 70% of the produced $ABTS^{\bullet-}$ radicals react with dissolved oxygen through reaction (8) (reaction (6):reaction (8) = 3:7). The theoretical stoichiometric factor for the conversion of ABTS to $ABTS^{\bullet+}$ is calculated to be 1.17 by summating reactions (3)–(6), (8) and (11) with the contribution ratio between reactions (6) and (8) being 3:7. The detailed calculation of the stoichiometric factors in condition 4 is presented in supplementary data, S-4.

In order to verify the stoichiometry between $[ABTS^{\bullet+}]$ and $\Delta[ABTS]$, several sets of experiments involving the photolysis of ABTS were performed under each of the aforementioned conditions (conditions 1–4), while measuring the variations in the absorbance of the ABTS solution at 340 and 415 nm. The concentrations of the ABTS molecules decomposed and the $ABTS^{\bullet+}$ radicals produced were then calculated based on the absorbance using Eqs. (1) and (2). However, to account for the partial conversion of ABTS to its protonated form, $HABTS^+$ at pH 3, a slightly decreased $\varepsilon_{ABTS,340}$ value of $3.37 \times 10^4\ M^{-1}\ cm^{-1}$ was used, which was calculated from the molar absorption coefficients of ABTS ($3.66 \times 10^4\ M^{-1}\ cm^{-1}$) and $HABTS^+$ ($9.13 \times 10^3\ M^{-1}\ cm^{-1}$), and the pK_a value of $HABTS^+$ (2.08) [14].

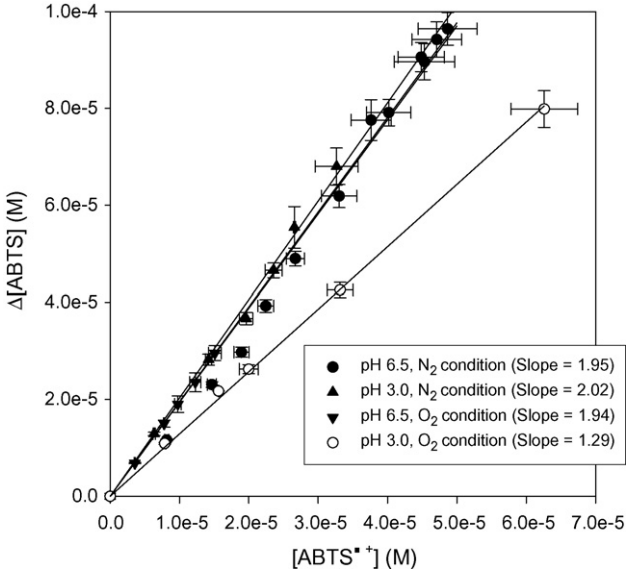

Fig. 9. Stoichiometries between the amounts of $ABTS^{\bullet+}$ produced and ABTS decomposed when solutions with a different pH and dissolved oxygen level were used, calculated from the results of Fig. 7.

Fig. 9 shows the linear plots of $[ABTS^{\bullet+}]$ against $\Delta[ABTS]$ during photolysis under conditions 1–4. The stoichiometric factors for the conversion of ABTS to $ABTS^{\bullet+}$ under each condition were obtained from the slopes of the linear plots. The values determined under conditions 1–3 were 1.95, 2.02 and 1.94, respectively, which was in agreement with the theoretical value of 2. The stoichiometric factor in condition 4 was measured to be 1.29, which was slightly higher than the theoretical value of 1.17. However, the obviously lower stoichiometric factor obtained under condition 4 supports the dual roles of $HO_2^{\bullet}/O_2^{\bullet-}$ proposed in this study.

4. Conclusion

The results obtained in this study can be summarized as follows. First, we demonstrated for the first time that ABTS in aqueous solution was directly photolyzed to yield its one-electron oxidized radical, $ABTS^{\bullet+}$, under UV irradiation at 254 nm. Spectrophotometric and spectrofluorometric data indicated that the one-electron transfer between the photo-excited and the ground-state ABTS molecules yielded $ABTS^{\bullet+}$ and the reduced form of ABTS, $ABTS^{\bullet-}$. Second, the photochemical production of $ABTS^{\bullet+}$ was strongly influenced by the pH of the solution used, as well as by the presence of dissolved oxygen. The formation of $HO_2^{\bullet}/O_2^{\bullet-}$ and their reactions with $ABTS/ABTS^{\bullet+}$ were suggested based on the pH-dependence of the quantum yields of the production of $ABTS^{\bullet+}$ in the presence or absence of dissolved oxygen, and observations from the UV/H_2O_2 experiments. The stoichiometry of $ABTS/ABTS^{\bullet+}$ strongly supported the proposed mechanisms.

The photochemistry of ABTS found in this study may be used as a simple chemical actinometry system in the UV–C region, since the photochemical oxidation of ABTS to $ABTS^{\bullet+}$ shows perfect linearity with respect to UV fluence (Fig. 7a and b). Additionally, the ability to perform a simple quantification of the produced $ABTS^{\bullet+}$ through spectrophotometric measurement of the UV–vis absorption spectrum is a strong advantage of this method. However, a more detailed investigation into other influences, such as temperature, light intensity and wavelength, is needed to evaluate the possibility of using ABTS photochemistry as a chemical actinometry system.

Acknowledgment

This research was partially supported by the Brain Korea 21 Program of the Ministry of Education. This support was greatly appreciated.

Appendix A. Supplementary data

Supplementary data associated with this article can be found, in the online version, at doi:10.1016/j.jphotochem.2007.12.030.

References

[1] B.S. Wolfenden, R.L. Willson, J. Chem. Soc., Perkin Trans. 2 (1982) 805–812.
[2] L.G. Forni, V.O. Mora-Arellano, J.E. Packer, R.L. Wilson, J. Chem. Soc., Perkin Trans. 2 (1986) 1–6.
[3] M. Erben-Russ, C. Michel, W. Bors, M. Saran, J. Phys. Chem. 91 (1987) 2362–2365.
[4] P. Neta, R.E. Huie, P. Maruthamuthu, S. Steenken, J. Phys. Chem. 93 (1989) 7654–7659.
[5] U. Pinkernell, H.-J. Lüke, U. Karst, Analyst 122 (1997) 567–571.
[6] Y. Lee, J. Yoon, U. von Gunten, Water Res. 39 (2005) 1946–1953.
[7] U. Pinkernell, B. Nowack, H. Gallard, U. von Gunten, Water Res. 34 (2000) 4343–4350.
[8] P. Maruthamuthu, D.K. Sharma, N. Serpone, J. Phys. Chem. 99 (1995) 3636–3642.
[9] C.A. Rice-Evans, N.J. Miller, G. Paganga, Free Radical Biol. Med. 20 (1996) 933–956.
[10] C.-H. Liao, M.D. Gurol, Environ. Sci. Technol. 29 (1995) 3007–3014.
[11] C.G. Hatchard, C.A. Parker, Proc. Roy. Soc. London A 235 (1956) 518–536.
[12] V. Balzani, V. Carassitti, Photochemistry of Coordination Compounds, Academic press, London, New York, 1970.
[13] H. Tamura, K. Goto, T. Yotsuyanagi, M. Nagayama, Talanta 21 (1974) 314–318.
[14] S.L. Scott, W.-J. Chen, A. Bakac, J.H. Espenson, J. Phys. Chem. 97 (1993) 6710–6714.
[15] B.H.J. Bielski, D.E. Cabelli, R.L. Arudi, A.B. Ross, J. Phys. Chem. Ref. Data 14 (1985) 1041–1100.
[16] R. Zellner, M. Exner, M. Herrmann, J. Atmos. Chem. 10 (1990) 411–425.
[17] X.–Y Yu, J.R. Barker, J. Phys. Chem. A 107 (2003) 1325–1332.
[18] G.V. Buxton, C.L. Greenstock, W.P. Helman, A.B. Ross, J. Phys. Chem. Ref. Data 17 (1988) 513–886.
[19] J.H. Baxendale, J.A. Wilson, Trans. Faraday Soc. 53 (1956) 344–356.